Ion beam production and study of radioactive isotopes with the laser ion source at ISOLDE

You may also be interested in:

Resonance laser ionization of atoms for nuclear physics
V N Fedosseev, Yu Kudryavtsev and V I Mishin

High efficiency resonance ionization of palladium with Ti:Sapphire lasers
T Kron, Y Liu, S Richter et al.

A complementary laser system for ISOLDE RILIS
S Rothe, B A Marsh, C Mattolat et al.

Collinear laser spectroscopy at ISOLDE: new methods and highlights
R Neugart, J Billowes, M L Bissell et al.

ISOLDE past, present and future
Maria J G Borge and Björn Jonson

Facilities and methods for radioactive ion beam production
Y Blumenfeld, T Nilsson and P Van Duppen

Three-step resonant photoionization spectroscopy of Ni and Ge
T Kessler, K Brück, C Baktash et al.

Production of negatively charged radioactive ion beams
Y Liu, D W Stracener and T Stora

Ion beam production and study of radioactive isotopes with the laser ion source at ISOLDE[*]

Valentin Fedosseev[1], Katerina Chrysalidis[1,2], Thomas Day Goodacre[1,3], Bruce Marsh[1], Sebastian Rothe[1] ⬤, Christoph Seiffert[1] and Klaus Wendt[2]

[1] CERN, Geneva, Switzerland
[2] Institut für Physik, Johannes Gutenberg-Universität, Mainz, Germany
[3] School of Physics and Astronomy, The University of Manchester, Manchester, United Kingdom

E-mail: Valentin.Fedosseev@cern.ch

CrossMark

Abstract

At ISOLDE the majority of radioactive ion beams are produced using the resonance ionization laser ion source (RILIS). This ion source is based on resonant excitation of atomic transitions by wavelength tunable laser radiation. Since its installation at the ISOLDE facility in 1994, the RILIS laser setup has been developed into a versatile remotely operated laser system comprising state-of–the-art solid state and dye lasers capable of generating multiple high quality laser beams at any wavelength in the range of 210–950 nm. A continuous programme of atomic ionization scheme development at CERN and at other laboratories has gradually increased the number of RILIS-ionized elements. At present, isotopes of 40 different elements have been selectively laser-ionized by the ISOLDE RILIS. Studies related to the optimization of the laser–atom interaction environment have yielded new laser ion source types: the laser ion source and trap and the versatile arc discharge and laser ion source. Depending on the specific experimental requirements for beam purity or versatility to switch between different ionization mechanisms, these may offer a favourable alternative to the standard hot metal cavity configuration. In addition to its main purpose of ion beam production, the RILIS is used for laser spectroscopy of radioisotopes. In an ongoing experimental campaign the isotope shifts and hyperfine structure of long isotopic chains have been measured by the extremely sensitive in-source laser spectroscopy method. The studies performed in the lead region were focused on nuclear deformation and

[*] This article belongs to the Focus on Exotic Beams at ISOLDE: A Laboratory Portrait special issue.

1

shape coexistence effects around the closed proton shell $Z = 82$. The paper describes the functional principles of the RILIS, the current status of the laser system and demonstrated capabilities for the production of different ion beams including the high-resolution studies of short-lived isotopes and other applications of RILIS lasers for ISOLDE experiments.

1. Introduction

The physical composition and intensity of ion beams, produced at radioactive ion beam facilities such as ISOLDE depends strongly on the type of ion source used to ionize the isotope of interest. At ISOLDE thick targets typically containing high-Z materials are used. Nuclear reactions induced by 1.4 GeV protons delivered from CERN Proton Synchrotron Booster accelerator yield a great variety of radionuclides. Often the isotope of interest is produced along with an overwhelming quantity of isobars which, if ionized, contaminate the ion beam transmitted through the ISOLDE mass separators. Therefore, a means of element selection in the extraction and ionization of radionuclides is often necessary if an isotope-pure ion beam is required.

At ISOLDE, the requirements for both selective and efficient ionization are largely fulfilled by the resonance ionization laser ion source (RILIS).

This ion source is based on the method of step-wise resonant excitation of atomic transitions by wavelength tuneable laser radiation: the laser wavelengths are precisely tuned so that the photon energies match successive electron transition energies of an ionization scheme as shown in figure 1. The valence electron is promoted to a high-lying energy level and then removed from the atom by a subsequent resonant step (via an autoionizing state), by non-resonant photoionization (to the continuum), or by collisional or field ionization (via a Rydberg level). Since each atomic element possesses a unique electronic energy level structure, the laser radiation interacts only with the chosen atomic species. The physics of the laser resonance photoionization process is described in the textbooks by Letokhov [1] and by Hurst and Payne [2]. In section 2.1 we will present only the basic considerations of laser–atom interaction relevant for efficient ionization.

An isobar-selective laser ion source based on laser resonant atomic photoionization was first proposed for on-line radioactive ion beam production at the 'On-line in 1985 and beyond—a workshop on the ISOLDE programme' event [3]. The technique was demonstrated at the Leningrad Nuclear Physics Institute (LNPI, now PNPI) in 1988 [4] and at ISOLDE in 1990 [5–7]. Based on these developments and the first application of the laser ion source in a physics experiment on radioactive ^{152}Ho at LNPI [8], the installation of a permanent laser ion source at the PS-BOOSTER ISOLDE facility was proposed to the ISOLDE Committee in 1993 [9].

Following this proposal, within a short period of time the laser ion source laboratory was established in the ISOLDE experimental hall. It was equipped with copper vapour lasers (CVL) and dye lasers, which, together with the necessary optical and mechanical components, were supplied by the Institute of Spectroscopy of the Russian Academy of Sciences (Troitsk, Moscow region) as a contribution to the ISOLDE programme. The first physics experiment to use the laser ion source was the study of neutron-rich silver isotopes [10] in 1994, during which the half-lives of $^{125-127}$Ag were determined. This success triggered
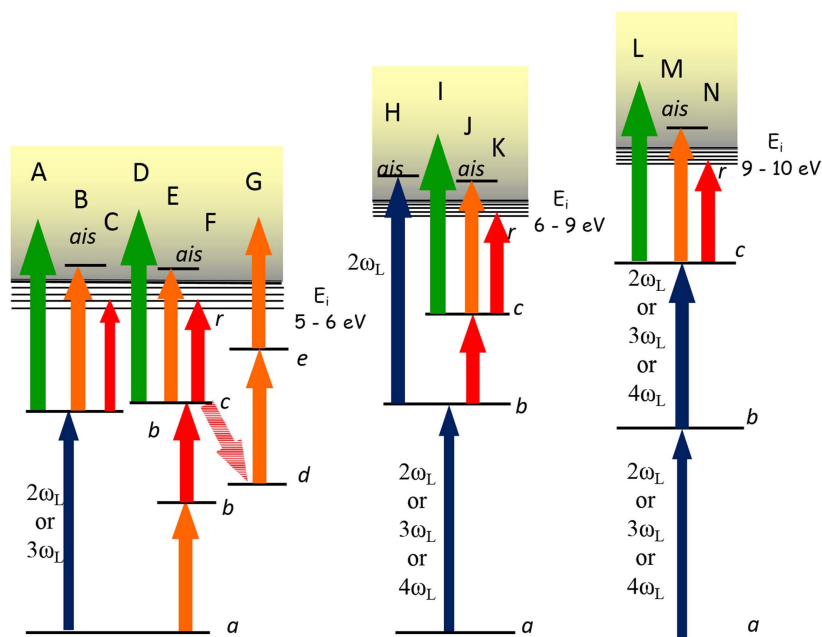
Figure 1. Resonance ionization pathways used by the ISOLDE RILIS. The laser configurations and number of transitions required are somewhat governed by the value of ionization potential E_i. The blue lines indicate transitions which require the generation of higher harmonics of laser radiation: frequency doubling ($2\omega_L$), tripling ($3\omega_L$) or quadrupling ($4\omega_L$).

several requests for other applications of the laser ion source by ISOLDE users. Laser ionized beams of Mn [11], Ni [12], Be, Zn, Cu and Cd [13] were produced at ISOLDE in the few subsequent years.

Using the CVL pumped dye laser system, isotopes of 26 different elements had been selectively laser-ionized at ISOLDE by the year 2007 [14]. Later on, the RILIS capabilities were significantly extended through several upgrades of the laser system, namely, a replacement of CVLs by Nd:YAG lasers [15], the installation of new commercial dye lasers and the addition of a complementary Nd:YAG-pumped Ti:Sapphire laser system [16, 17]. Today, the RILIS installation is a versatile, remotely-operated, dual laser system comprising state-of–the-art solid state and dye lasers capable of generating multiple high-quality laser beams at any wavelength in the range of 210–950 nm [18]. The current list of ion beams available for production at ISOLDE using the RILIS includes 40 elements (see section 4.1 for details). In section 2 we describe the basic principles of the RILIS method including the ionization process in a hot tubular metal cavity and the laser system itself. Newly developed approaches, such as the laser ion source and trap (LIST) [19] and the versatile arc discharge and laser ion source (VADLIS) [20] are described in section 3. Section 4 is devoted to RILIS applications which, in addition to the standard mode of RILIS operation for efficient and selective ionization of a requested element, includes the operation of the RILIS lasers in a high-resolution mode for laser probing of different isotopes and nuclear isomers of the chosen element. This highly sensitive laser spectroscopy method for the study of unstable isotopes

was pioneered at LNPI [21]. At ISOLDE it was further developed as the 'in-source resonance ionization spectroscopy (RIS)' method [22] and applied in a number of experiments for the study of nuclides far from stability. Examples of this application are presented in section 4.3. The concluding section contains a review of current work on RILIS development and outlook to future extension of RILIS capabilities and applications at ISOLDE.

2. RILIS method

2.1. Laser resonance ionization of atoms

A free atom can be excited and ionized with a high probability through a resonant interaction with the radiation from a series of pulsed lasers tuned to match the energy of consecutive transitions between atomic states. Figure 1 illustrates the typical schemes of resonance excitation and ionization used by the RILIS.

Each atomic transition between bound states *a* and *b* (for schemes depicted in figure 1 this could be applied also for transitions b-c, c-r and d-e), can be characterized by an absorption cross section

$$\sigma_{ab} = \frac{g_a}{g_b} \frac{\lambda_{ab}^2}{4\pi^2} \frac{A_{ba}}{\Delta \nu_t^{ab}},\tag{1}$$

where g_a and g_b are the degeneracy of the levels *a* and *b* respectively, λ_{ab} is the wavelength of the illuminating laser, A_{ba} is the Einstein coefficient and $\Delta \nu_t^{ab}$ is the spectral width of the transition between states *a* and *b* in the laser atom interaction region. The kinetics of multi-step excitation and ionization can be modelled by simple rate equations. By solving the equation system for atomic levels interacting with laser light and integrating the ion production over the pulse duration one can obtain the ionization efficiency η_{lp} resulting from a single act of excitation and ionization by synchronized laser pulses of given duration t_{Lk} and energy density $\mathcal{E}_k$ (here index *k* refers to a step number in the excitation process). The dependence of the η_{lp} versus laser energy density reveals that an efficiency saturation is possible. The use of short laser pulses for resonant excitation minimizes the losses due to the spontaneous decay of excited atomic states. If $t_{L1} < \tau_b$ (τ_b is the decay time of the excited state *b*) the laser pulse energy density required for saturation of the resonant transition between bound states is linked to its cross section as

$$\mathcal{E}_{ab}^{\text{sat}} = \frac{h\nu_{ab}}{2\sigma_{ab}} \frac{\Delta \nu_L^{ab}}{\Delta \nu_t^{ab}},\tag{2}$$

where *h* is the Planck constant, ν_{ab} is the frequency of the laser light and $\Delta \nu_L^{ab}$ is the spectral line width of the laser driving the transition. A complete spectral coverage of the available atoms is required in order to maximize the efficiency of a resonant excitation, i.e.

$$\Delta \nu_L^{ab} \geqslant \Delta \nu_t^{ab}.\tag{3}$$

The absorption cross sections of allowed electric dipole transitions between bound atomic states typically have values in the range of $\sim 10^{-10}$–$10^{-15}\,\text{cm}^2$. Saturation can therefore be achieved using a nanosecond-scale laser pulse length with an energy density in the range of $\sim 10^{-6}$–$10^{-3}\,\text{J cm}^{-2}$.

Transitions to the ionization continuum are much weaker, with absorption cross sections in the range of $\sigma_i \leqslant 10^{-17}\,\text{cm}^2$. Correspondingly, a higher energy density is required to saturate such an ionizing transition, which for laser pulse at the light frequency ν_i is defined as

$$\mathcal{E}_i^{\text{sat}} = \frac{h\nu_i}{\sigma_i}. \tag{4}$$

The ionization efficiency of schemes using transitions to the continuum (paths A, D, I, L on figure 1) is usually limited by the laser pulse energy available for the last step. Using schemes with transitions to autoionizing or highly excited Rydberg states is advantageous since the cross sections are typically 2–3 orders of magnitude larger than those of non-resonant transitions to the continuum.

Autoionizing states ('ais' in figure 1) are the bound atomic states lying above the ionization threshold which exist in multi-electron atoms due to an excitation of two or more electrons. Each of these electrons undergo a transition between discrete quantum states so that the total excitation energy of the atomic system exceeds the ionization limit. This energy can then be quickly redistributed between the excited electrons in a non-radiative process which results in to the emission of a free electron and leaves the atom in an ionic state. Schemes with 'ais' excitation are indicated in figure 1 by letters B, E, H, J, M.

Not all atoms possess autoionizing states conveniently accessible by the RILIS laser tuning range. However, practically any atom can be excited to levels with high principal quantum numbers n lying in the vicinity of the ionization threshold, the so called Rydberg levels. Since the energy required for ionization of Rydberg atoms is very small (order of meV), ionization of atoms excited to such states can be efficiently driven by an interaction with an external electric field, black-body radiation or collisions with other particles. Ionization schemes involving Rydberg states are presented in figure 1 by the letters C, F, K, N. In practice, the use of such schemes at the RILIS is not routinely practiced due to the limited power output of an additional laser beam at the required wavelength. Furthermore, the lack of precise control of the ionization mechanism of Rydberg atoms adds an element of uncertainty regarding the reproducibility of the performance of such ionization schemes.

Nevertheless, in certain cases where the alternative approach of using a high power 532 nm laser beam for non-resonant ionization results in an unacceptable increase in background due to enhanced ionization of molecular beam contaminants, the use of a Rydberg or autoionizing state can achieve a higher degree of ion beam purity without significantly compromising ionization efficiency.

2.2. Ionization in a hot cavity

The ISOLDE RILIS lasers operate at a pulse repetition rate of $f = 10\,\text{kHz}$ and perform ionization of atoms inside a hot cavity: a refractory metal tube, with an internal diameter $d = 3$ mm and length $L = 34$ mm that is typically heated to $\sim$2000 °C. The heating method is resistive, resulting in a longitudinal electrical potential. This potential accelerates ions created inside the hot cavity towards the extraction aperture. The cavity is connected to the target container where the radio-isotopes are produced. The laser beams are directed along the axis of the cavity from the ion extraction site as depicted in figure 2.

The hot cavity concept was developed to enable efficient ionization of a continuous supply of atoms moving in a vacuum through the path of pulsed laser beams. The geometry of the cavity provides confinement of atoms within the laser beam during the time interval between consecutive laser pulses while the hot environment prevents adsorption of non-volatile species on the internal cavity walls. In addition, ions created in the hot cavity are confined due to the negative plasma sheath potential caused by a thermal electron emission of the cavity walls [23]. The nature of ion confinement and extraction in the hot cavity is identical to that of thermal ion sources that have been developed and used at isotope separators many years [24–28].
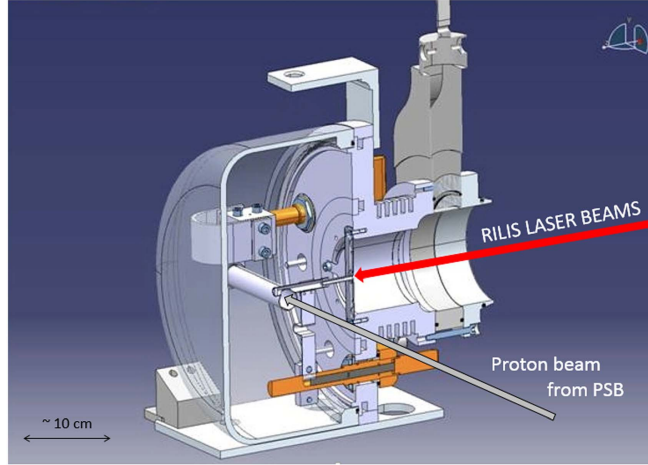
Figure 2. Target and hot cavity ion source assembly.

Atoms with a relatively low ionization potential $E_i \leqslant 6\,\text{eV}$ can be surface ionized quite efficiently in the hot cavity. Fundamentally this process is independent of the element-selective resonance laser ionization process but it is the principal source of isobaric impurity of RILIS ion beams. It is possible to optimize the design and operating conditions of the RILIS hot cavity to minimize the contribution of thermal ionization while preserving its ion confinement properties. In particular, the surface ionization degree α_s strongly depends on the wall temperature T as derived from the Saha–Langmuir equation

$$\alpha_s = \frac{n_{is}}{n_{0s}} = \frac{g_i}{g_0} \exp\left(\frac{\phi - E_i}{kT}\right), \tag{5}$$

where n_{is} and n_{0s} are concentrations of ion and neutrals near the surface, g_i and g_0 are the statistical weights of the ionic and atomic ground states, ϕ is the work function of the electron emitting surface. The surface ionization efficiency β_s is defined then as

$$\beta_s = \frac{n_{is}}{n_{is} + n_{0s}} = \frac{\alpha_s}{1 + \alpha_s}. \tag{6}$$

In a hot cavity with small exit aperture atoms collide with the surface many times which, under the assumption of a non-zero probability of ion survival and extraction from the cavity volume, will result in a higher ionization efficiency than defined by (5) and (6). The expression for the resulting cavity ionization efficiency η_s has been proposed in [28] taking into account the mean number of collisions of atoms with the walls κ and the probability γ of an ionized particle to leave the cavity as ion:

$$\eta_s = \frac{\beta_s \gamma \kappa}{1 - \beta_s (1 - \gamma \kappa)}. \tag{7}$$

The survival of ions inside the cavity is supported by the negative plasma sheath potential Φ_p which has been derived in [23] from the Boltzmann relation for charge densities at the wall and inside the cavity volume in the form

$$\Phi_p = \frac{kT}{2e} \ln\left(\frac{n_{is}}{n_{es}}\right), \tag{8}$$

where e is the electron charge and n_{es} is the concentration of electrons near the surface which is governed by Richardson's law

$$n_{\mathrm{es}} = 2\left(\frac{2\pi mkT}{h^2}\right)^{3/2} \exp(-\phi/kT). \tag{9}$$

Obviously, the contribution of surface ionization could be reduced by decreasing the temperature. In addition, using low work function materials for cavity walls is helpful both for decreasing surface ionization and for increasing the depth of plasma potential due to a more intense emission of electrons at a given temperature. The effect of work function on the laser/surface ionization ratio has been demonstrated experimentally in [7, 29]. It is also known that the RILIS selectivity can be improved by operating the cavity at a reduced temperature. However, at too low ion source temperature the reduced plasma potential results in an increased probability of recombination of laser ions at the walls, thereby decreasing the laser ion source efficiency. One must also consider the temperature-dependence of wall sticking times, which can impair the ion source efficiency of non-volatile species with short half-lives, but which will not be apparent when optimizing the ion source for a stable isotope.

For efficient laser ionization in a hot tubular cavity the diameters of laser beams are to be adapted to the ion source internal diameter as to completely fill the internal volume of the source. In this case the laser ionization efficiency can be estimated as

$$\eta_{las} = \frac{\gamma\eta_{1l}f}{\gamma\eta_{1l}f + (2/3)(d/L^2)\bar{v}}, \tag{10}$$

where $\bar{v}$ is the mean thermal velocity of atoms. This expression is obtained assuming a linear decrease of the atom number density along the tube with $L \gg d$ [30].

The ion extraction probability γ depends on the strength of electrical field created by resistive heating of the cavity and the value of plasma sheath potential (8). It is important to note that macroscopic presence of positively-ionized impurities can significantly influence the plasma sheath [23]. Species with a low ionization potential are therefore especially harmful as their ion density near the surface can exceed the electron density, thereby changing the sign of Φ_p to positive. In this case the ion confinement mechanism does not work anymore. On several occasions a drastic reduction of laser ion yield has been observed following an uncontrollable release from mass markers charged with high-capacity alkali dispensers.

2.3. RILIS laser system

One of the valuable operational advantages of using the laser ionization for production of radioactive ion beams is the possibility to situate the lasers and most of the associated laser beam control equipment outside of the radioactive target and separator areas. This facilitates any work on setup and maintenance of the technically complex laser systems since the access to the laser installation is not affected by the protons-on-target operation. At ISOLDE the RILIS laser cabin is located inside the experimental hall on a platform above the ion beam lines and the entrance door to the high resolution separator (HRS) area as depicted in figure 3.

This location enables laser beam transport to the front-ends of either of the ISOLDE separators (see figure 3). The required combinations of laser beams are generated inside the laser laboratory (RILIS cabin in figure 4) and directed to one of the two exit ports. Further on, the laser beams are transported within metal tubes and steered towards the mass separator using 40 × 40 mm fused-silica right-angle prisms. The final prism of each laser path is installed opposite to the window of the mass separator vacuum chamber, intercepting the line-of-sight to the ion source extraction aperture. The lengths of the optical paths from the laser cabin to an ion source position are 18 m and 23 m for GPS and HRS respectively.

An additional optical beam path from the RILIS cabin has been established to enable laser-access to the ISOLDE RF cooler and buncher, ISCOOL, which is installed downstream of the HRS. A laser beam from RILIS can be injected into the ISCOOL through a window in
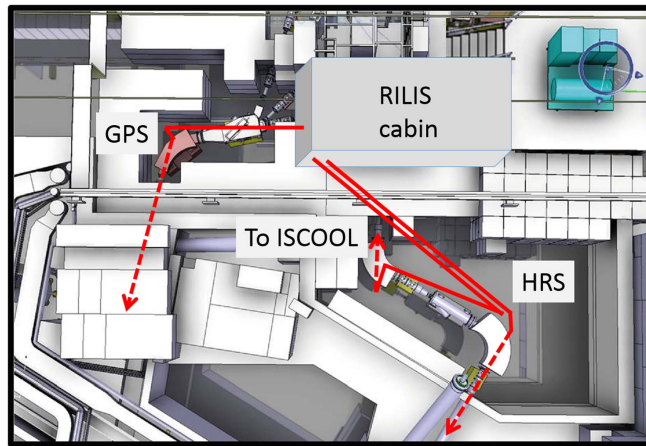
Figure 3. Schematic view of RILIS laser cabin location in ISOLDE experimental hall. Laser beam transport optics are installed in the areas of the general purpose separator (GPS) and the HRS to direct the laser radiation to the respective ion source or to the linear gas-filled Paul trap ISCOOL.
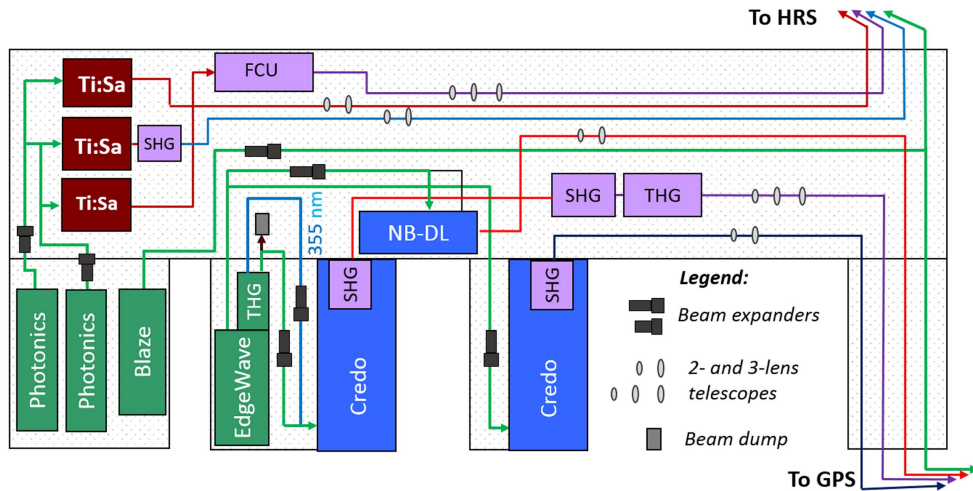
Figure 4. Layout of the RILIS laser installation. Three Ti:sapphire lasers (Ti:Sa) are pumped by two Photonics Nd:YAG lasers; two Credo and one narrow-band (NB-DL) dye lasers are pumped by the EdgeWave Nd:YAG laser; the beam from the Blaze Nd:YVO$_4$ laser is directed to the ion source of either GPS or HRS separator. Frequency conversion (up to 4ω) is performed using modules for second harmonic generation (SHG), third harmonic generation (THG) and a frequency conversion unit (FCU). Mirrors and other optical elements for splitting and transporting laser beams are not shown for simplicity.

the 60° magnet. Laser–ion interactions inside ISCOOL have so far been exploited for optical pumping of manganese ions to a metastable state of the ion for a laser spectroscopy study at the COLLAPS experiment [31]. Further applications of this laser access point, such as laser-induced molecular breakup, are foreseen.

During on-line ISOLDE operation the mass separator areas are not accessible because of a high ambient radiation dose rate. However, all required manipulations with lasers beams, including the setup and maintenance of the laser installation can be safely performed inside the laser cabin, which is shielded from the adjacent mass separator areas by $\geqslant 80$ cm thick concrete walls.

The principal components of RILIS installed in the laser cabin are following:

- Laser installation with optics for distribution and shaping of laser beams (see figure 4).
- Instruments for measuring the properties of laser radiation, in particular average power, wavelength, linewidth, pulse duration, beam profile.
- Opto-mechanical systems for launching and precise alignment of laser beams into the ion source cavities of either GPS or HRS front-ends as well as to the linear gas-filled RFQ trap for ion beam cooling and bunching ISCOOL installed at the exit of HRS.
- Opto-mechanical system and instrumentation for observation of reference laser beams, which are representative in size, shape and relative positions of the overlapping laser beams at the ion source location.
- FPGA-based RILIS machine protection system (RMPS) to detect potentially hazardous operational faults in the laser system [32]. This reacts automatically to prevent such equipment damage by taking the appropriate laser equipment control function and alerting the laser operator.
- Atomic beam unit [33] for reference measurements of ion signals and development of ionization schemes.

The layout of RILIS laser installation is depicted in figure 4. The laser setup includes wavelength-tuneable lasers based on two different types of the gain medium: liquid solutions of organic dyes and solid state titanium-doped sapphire crystals (Ti:Sa, chemical formula $Ti^{+3}:Al_2O_3$).

A selection of ~ 15 laser dyes are available for operation of the dye lasers with 355 or 532 nm pumping. Each kind of dye molecule has a specific range of absorption and emission. Liquid solution of a laser dye typically enables a 20–50 nm wide laser tuning range. For dye laser pumping a green beam at 532 nm, or a UV beam at 355 nm is available: the frequency-doubled and tripled output of the 10 kHz Nd:YAG INNOSLAB laser (EdgeWave GmbH, model CX16III-OE). The overall tuning ranges possible from the selection of laser dyes using green or UV pumping are 540–860 nm and 390–580 nm respectively. The residual beam at the fundamental wavelength 1064 nm currently is not used and dumped externally. A RILIS upgrade in 2010 included the replacement of the home-made dye lasers with commercial dye lasers supplied by Sirah Lasertechnik GmbH (model Credo Dye) and the narrow-band dye laser supplied by DMK Laser Microsystems Co. Ltd (Russia). The latter contains a Fabry–Perot etalon inside the resonator, which reduces the laser line width to 0.8 GHz. By removing the etalon the laser can be switched to a broad line width mode of operation.

The suite of Ti:Sa lasers was installed at RILIS as a complementary system to the dye lasers [16, 17]. These lasers offer a broad tuning range of 680–950 nm in the infrared part of optical spectrum extendable to 210–475 nm by harmonic generation. Pumping of the Ti:Sa lasers is performed by the green 532 nm beams of two intra-cavity frequency-doubled Nd:YAG lasers (Photonics Industries International Inc., model DM-60-532). A narrow linewidth operating mode of the Ti:Sa laser has been developed [34, 35] to satisfy the requirements of the in-source RIS and nuclear isomer selectivity.

Figure 5 presents the approximate wavelength tuning curves of RILIS lasers. The output power at fundamental wavelength emitted by dye lasers in the visible range is in general higher than that of the Ti:Sa lasers in IR because the dye lasers are equipped with
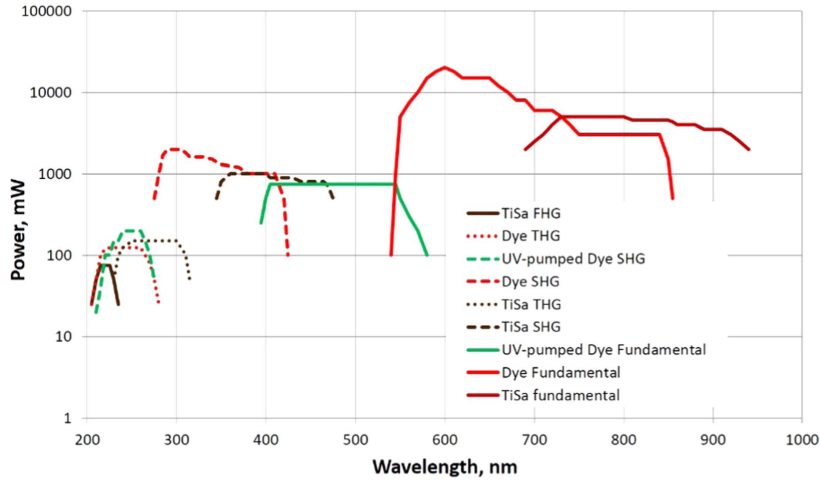
Figure 5. Wavelength tuning curves of the RILIS dye and Ti:Sa lasers including frequency multiplication by second harmonics generation (SHG), third harmonics generation (THG) and fourth harmonics generation (FHG).

amplification stages which can accept a higher pumping power (up to a total of 60 W per laser). For Ti:Sa lasers the pumping power is limited to approximately 20 W by the damage threshold of Ti:Sa crystal, the cavity optics and by thermally-induced laser output instabilities.

The most recent addition to the system of RILIS lasers is the frequency-doubled Nd:YVO$_4$ Blaze 532-40-HE laser (built by Lumera Laser GmbH and supplied via Coherent Inc.), which emits a high quality TEM$_{00}$ beam at 532 nm. As it was demonstrated in [36], this laser beam has an excellent focusing capability thus enabling a twofold increase of ionization efficiency for schemes with non-resonant transitions at the last step. The Blaze laser can also be used for pumping the dye lasers.

All pump lasers and the Blaze laser are operated synchronously at the pulse repetition rate of 10 kHz.

Multiple synchronized 10 kHz triggering signals, each with appropriate logic, widths and adjustable delays are provided by a Quantum Composers 9538 8-channel digital delay pulse generator.

The key parameters of RILIS lasers are summarized in table 1.

The transverse dimensions of each pumping beam are modified using spherical lens beam expanders adjusted so as to match the requirements of the Ti:Sa and dye lasers. Expanders with a fixed 3× expansion factor have been chosen for the Photonics beams used to pump Ti:Sa lasers. Variable 2×–8× beam expanders with anti-reflection coating for 532 and 355 nm are installed in the beams of EdgeWave and Blaze lasers.

The focusing of the RILIS beams into the ion source cavity is achieved using telescopes installed in the laser cabin at appropriate distances from each corresponding laser. For the focusing of a real laser beam over a long distance L the telescope has to be configured to ensure a sufficiently large beam diameter D on its exit lens which can be defined from the relation between the beam radius at waist w_0, laser light wavelength λ and beam quality factor M^2:

$$2w_0 = M^2 \frac{4\lambda}{\pi} \frac{L}{D}. \tag{11}$$

Since the RILIS lasers do not produce ideal Gaussian beams, M^2 may be large, therefore a beam expansion to a diameter of 10–20 mm at the launch point in the laser laboratory is

Table 1. Key parameters of RILIS lasers.

Laser source	Wavelength, nm	Max. power, W	Pulse duration (FWHM), ns	Line width, GHz
Nd:YAG *EdgeWave CX16III-OE*, beam A	532	80	8	
Nd:YAG *EdgeWave CX16III-OE*, beam B	532	40	9	
Nd:YAG *EdgeWave CX16III-OE*, beam C	355	20	11	
Nd:YAG *Photonics DM-60-532* (2 units)	532	60	130–170	
Nd:YVO$_4$ *Coherent Blaze 532-4-HE*	532	40	17	
Dye laser *SIRAH Credo* (2 units)	390–860	20	7	12
Narrow-band dye laser *DMK Microsystems*	390–860	10	10	0.8 or 15
Ti:Sa laser (3 units, narrow-band option)	680–950	6	30–50	0.8 or 5
Second harmonic of dye lasers	215–425	2	6	
Second harmonic of Ti:Sa lasers	340–475	1	∼30	
Third harmonics of dye lasers	210–270	0.2	5	
Third harmonics of Ti:Sa lasers	235–315	0.15	∼30	
Fourth harmonics of Ti:Sa lasers	210–235	0.15	∼30	
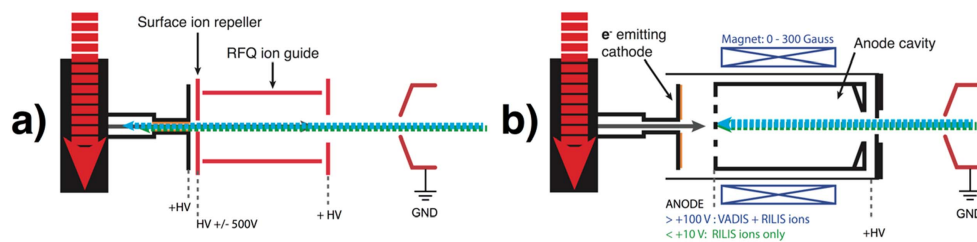
Figure 6. Alternatives to the hot-cavity laser ion source at ISOLDE. (a) The LIST for high selectivity through active surface ion suppression, (b) the VADLIS, the most versatile ion source option at ISOLDE.

typically required to achieve a laser beam waist similar in size to the 3 mm diameter aperture of the ion source cavity. For round beams the telescopes are composed of two spherical lenses, while for elliptical beams, which are usually produced in the process of harmonic generation, telescopes including cylindrical and spherical lenses are used to optimize the aspect ratio.

Up to four laser beams can be simultaneously launched to the GPS or HRS area using a set of closely mounted dielectric mirrors located next to the laser beam exit ports of the RILIS room. The beams pass through a fused silica wedged plate installed at the half-way point of the optical path to the ion source. This generates two spatially separated ≈4% reflections which are directed back to the reference beam observation system situated in the laser room. For other RILIS applications, discussed in section 4.4, it is also possible to transmit a laser beam to the ISCOOL ion beam cooler-buncher or to the GLM beam line inside the ISOLDE hall. An optical fibre link also exists for beam transport to and from the laser laboratory of the collinear resonance ionization spectroscopy (CRIS) experiment. A detailed description of most aspects of the RILIS laser installation can be found in [18].

3. New concepts of laser ion sources at ISOLDE

3.1. Ion source for highest selectivity: LIST

The LIST was developed as a means of applying the RILIS technique whilst achieving orders-of-magnitude suppression of thermal ions from the ISOLDE target, transfer line and hot-cavity assembly. As can be seen in figure 6, the LIST consists of three main components:

- *Ion repeller*. Situated immediately downstream of the hot cavity exit, the repeller, operating in the range of $+/-500$ V, enables switching between 'ion guide' ($-$ve polarity) and 'LIST mode' ($+$ve polarity) to either extract or repel ions emerging from the hot-cavity.
- *RFQ ion guide*. The RFQ ion guide (1 MHz, 500 V p-p) positioned immediately after the repeller and on-axis with the hot cavity, provides transverse confinement of ions drifting along the length of the LIST.
- *LIST end plate*. This aperture, which is the end plate of the LIST structure, opposite to the repeller, is required to screen the LIST volume from the electrical potential of the grounded extraction electrode. This ensures that laser-ions created inside the LIST do not suffer from an energy spread that would be incompatible with the subsequent isotope-selective mass separation of the ion beam.

Table 2. A compilation of surface-ion suppression factors measured during off-line and on-line operation of the ISOLDE LIST.

Isotope	Ion current or count rate		Unit	Suppression factor
	Ion guide mode	LIST mode		
^{23}Na^{offline}	75	0.4	pA	200
^{48}Ti^{offline}	145	Bg	pA	$>10^3$
^{174}Yb^{offline}	3	Bg	pA	$>10^2$
^{26}Na	75 000	Bg	$\beta/\mu C$	$>10^5$
^{30}Na	1400	Bg	$\beta/\mu C$	$>10^4$
^{46}K	13 000	Bg	$\beta/\mu C$	$>10^5$
^{205}Fr	610 000	25	$\alpha/$supercycle	2500
^{212}Fr	80	2	pA	70
^{220}Fr	15 000	Bg	$\alpha/$supercycle	$>10^3$

The letter T ('trap') of the LIST acronym is somewhat misleading since the LIST offers only two-dimensional (transverse) confinement of ions and therefore acts as an ion guide, rather than as an ion trap. At the ISAC-TRIUMF facility, this distinction has been acknowledged by the use of the IG-LIS (ion guide laser ion source) acronym [37], although this name has the potential to be confused with that of the IGLIS (in gas laser ionization and spectroscopy) method used at gas-catcher ISOL facilities.

The LIST name is in fact inherited from the initial concept of the LIST as a miniature gas-filled Paul trap, proposed by Blaum *et al* in 2003 [38]. To meet the durability, efficiency and reliability demands of the on-line ISOLDE target assembly, this initial LIST concept was greatly simplified towards its current form. This work was conducted by a CERN/Mainz collaboration led by the LARISSA group of Wendt and was the subject of several PhD theses [39–41]. Some key functionality (ion beam cooling and bunching) first proposed by Blaum has therefore been lost whilst the primary function of achieving orders-of-magnitude selectivity improvements has been demonstrated under normal on-line operating conditions with a UCx target [42]. So far the LIST has been successfully used for the production of pure Mg [19] and Po [42, 43] beams. Table 2 is a summary of the LIST suppression factors that have been measured during off-line and on-line operation at ISOLDE. In many cases the LIST-mode surface ion rate was below the detection limit of the device used for determining the ion rate. In these cases, it is only possible to state a lower limit of the suppression factor. For the most recent LIST device, which was built with the minimum acceptable distance of the LIST repeller from the hot cavity exit of 1 mm, the estimated RILIS efficiency loss factor was 20. This was determined by comparing the LIST mode and ion guide mode RILIS ion rates.

3.2. Hybrid plasma-laser ion source: VADLIS

The VADLIS [20] has become an established ion source option at ISOLDE in recent years. Currently this approach makes use of a standard ISOLDE FEBIAD (the VADIS) ion source [44] as a laser–atom interaction volume, as seen in figure 6(b). When operating at low anode voltage (<10 V), and with optimized cathode and magnetic field settings, the FEBIAD cavity becomes an effective environment for selective laser resonance ionization. In the numerous off-line and on-line tests, under standard operating conditions, a RILIS-mode efficiency typically equal to or greater than the FEBIAD-mode efficiency for the element of interest has been obtained.

To date, the VADLIS has been applied at ISOLDE for resonance ionization of Ga, Mo, Ba, Hg, Mg and Cd. For the latter three, this involved on-line operation for the production of radioisotopes.

The examples of Hg, Mg, Ba and Mo highlight several of the unique capabilities of the VADLIS ion source:

Hg—The highest intensity neutron-deficient mercury beams at ISOLDE have been produced using lead targets. The molten lead bath target is attached to the ion source via a spiral, temperature-controlled chimney (lead vapour condenser), which is currently only compatible with FEBIAD-type ion sources. The VADLIS is therefore currently the only option for achieving selective resonance laser ionization of isotopes from molten targets. In 2015, a campaign to study both neutron deficient and neutron rich mercury isotopes by in-source RIS was, in fact, the first on-line application of the VADLIS for a physics experiment [45].

Mg—During 2016, an ISOLTRAP experiment aimed to study ^{21}Ne and ^{23}Mg isotopes in the same experiment using a SiC target coupled to a VD5 VADIS [46]. On account of their atomic structure and high ionization potential, noble gases ions cannot be created by the surface or RILIS ion sources, hence the FEBIAD-type source is required for this experiment. Under normal operation, the isobaric background generated at mass 23, (predominantly ^{23}Na), proved overwhelming for the successful ^{23}Mg. The use of the VADLIS method enables quick switching to the RILIS-mode of VADLIS operation, significantly enhancing the ^{23}Mg beam intensity whilst providing a moderate suppression of ^{23}Na and orders-of-magnitude suppression of all other background isobars.

Ba—On account of the relatively low ionization potential of barium (5.21 eV), barium beams can be efficiently produced at ISOLDE using a surface ion source operating at high temperature (>2000 °C). Under these conditions the beam purity for radiogenic Ba$^+$ is typically poor due to the readily surface-ionized contaminants: mainly caesium and indium isobars. Fluorination of the target material can address this, resulting in the creation of BaF$_2$, which is extracted as BaF$^+$ from a FEBIAD source. This has proven effective for the purification of neutron-deficient barium beams produced from lanthanum targets since BaF$^+$ ions occupy a mass region devoid of isobaric contamination. For neutron-rich Ba beams however, a UCx target is required. In this case the abundantly produced europium and samarium isotopes appear as isobaric contaminants in the extracted BaF$^+$ beams. As an alternative approach, an optimal laser ionization scheme for atomic barium has been developed and tested in combination with both the hot-cavity and the VADLIS ion sources. Since the anode grid of the VADIS cavity is positively charged, surface ions created in the hot cathode region are actively repelled. Furthermore, unlike the situation for the hot cavity RILIS, RILIS-mode VADLIS laser ion survival is not reliant on electron emission from the cavity walls. Neglecting condensation/wall sticking considerations, optimal RILIS efficiency can therefore be achieved at a lower temperature, further reducing the surface-ionized proportion of the extracted ion beam. The VADLIS therefore offers the possibility to increase the selectivity of the laser ion source. A comprehensive Ba$^+$ ion yield assessment is required to fully validate this approach however, in offline tests a Ba$^+$ laser to surface ion ratio of 8 has been achieved in the VADLIS (compared to 1 for hot-cavity RILIS) under typical operating conditions. A further increase in selectivity could be realised through the use of an anode cavity made from a low-work function material.

Mo—A resonance ionization scheme for the refractory metal molybdenum was developed in an off-line test at ISOLDE by RIS using the RILIS in 2016. On account of the low vapour pressure at the typical ion source operating temperature, speculative ionization scheme development for elements such a Mo is challenging in the absence of any means of assessing

the presence of a sufficient supply of the atoms of interest. By offering the possibility of easy switching between RILIS and VADIS ionization modes the VADLIS removes this degree of uncertainty: a VADIS-mode Mo ion current was first established, demonstrating the availability of a suitable quantity of Mo atoms. Then, after switching to RILIS-mode, the spectroscopic search for Mo ionization schemes could begin with a pre-established knowledge of the availability of the sample as well as a reference value for the expected ion rate.

4. RILIS applications

4.1. Ion beam production

The principal application of RILIS is the production of ion beams of elements required for ISOLDE experiments. As the isotopic selectivity provided by the mass-separation in most cases is sufficient for the purpose of an experiment, laser ionization is required to be only an element-selective process. Moreover, when the hyperfine splitting of the ground atomic state exceeds the spectral width of applied laser light, a significant fraction of atoms may not interact with the laser radiation, thus reducing the ionization efficiency. Therefore, whenever possible the spectral bandwidth of laser radiation should be sufficiently broad in order to cover the hyperfine structure. In addition, using such broad-band laser radiation facilitates studies of long isotopic chains by reducing the sensitivity of ionization process to the isotope shift of resonant atomic transitions.

Effective ion beam production requires stable laser performance during round-the-clock operation. Until 2014 this was ensured by continuous supervision of the RILIS installation by laser experts working in shifts. In order to facilitate both laser operation and performance monitoring, a comprehensive LabVIEW-based system of remote control and equipment monitoring of RILIS has been developed [32, 34, 47, 48]. It is known as REACT: the RILIS equipment acquisition and control tool. Due to this development complemented by the implementation of the machine protection system RMPS, autonomous functioning of RILIS during normal operation became safe and reliable. Thus, the goal of a transition from the shift-based to the on-call-based operation has been achieved.

In general, the purity requirements for specific isotopic beams specify directions of laser ionization scheme development, while wavelength and power capabilities of the RILIS laser system define the range of elements accessible for efficient laser ionization. Most of the elements in the Periodic table could potentially be resonantly excited and ionized using the RILIS lasers system. However, the range of ion beams at ISOLDE is defined by the production and release properties of ISOLDE targets. In particular, radioactive isotopes of refractory metals are not released as free atoms at the target temperature $\leqslant 2200\,°C$. Therefore, the RILIS is applied mainly to the more volatile elements with resonant transition wavelengths above 210 nm.

The list of elements ionized with RILIS at ISOLDE is presented in table 3. It includes information about the applied ionization schemes with an indication to the specific type of excitation pathway illustrated in figure 1. Whenever available, the data on ionization efficiency are included. These are absolute efficiency measurements made using calibrated samples and/or relative values of laser ion current observed in comparison with a surface ion current under typical operational parameters of the hot cavity ion source. The last column of table 3 gives references to first publications on the specific scheme development or application. Some additional details (lasers used, dyes) can be found in [18].

Table 3. RILIS ionization schemes applied at ISOLDE.

Element	Type of scheme[a]	λ_1 (vac) nm	λ_2 (vac) nm	λ_3 (vac) nm	Efficiency Abs. %	Efficiency Laser/ surf.	Isotopes A	Reference
Li	D	670.96	610.53	532		0.6	6–11	[49]
Be	H	234.93	297.41	—	>7		7, 9–12, 14	[13]
Mg	I	285.30	552.99	510.69 & 578.37 532	10		21–35	[50] [15]
Al	A	308.30 & 309.37	510.69 & 578.37 532	—	>20	100	26–36	[51] [18]
Ca	J	422.79	585.91	655.18		300	40–54	[40, 52]
Sc	I	327.46	720.03	510.69	15	400	Stable	[53]
Cr	J	357.97	698.03	579.31	~20	2200	48–63	[49, 54]
Mn	J	279.91	628.44	510.69 647.52	19		48–69	[11] [15]
Fe	L	372.10	321.26	532		10^5	54–62	[55]
Co	I	304.49	544.61	510.69 & 578.37	>4		Stable	[51]
Ni	J	305.17	611.28	748.42	>6	8000	56–70	[12]
Cu[e]	I	327.49	793.53	510.69	6.6		57–78	[13]
	H		287.98	—	>7			[56]
Zn	I	213.92	636.41	510.69 532	5		58–82	[13] [15]
Ga	A	287.51 287.51 & 294.50	510.69 & 578.37 532	— —	21	20–30 >100	61–86	[57] [14]
Ge	I	275.54	569.35	532	>2		Stable	[49, 58]
Y	I	408.49 414.40	582.07 662.55	582.07 510.69		16 88	Stable	[51] [53]
Mo	M	379.93	415.91	635.16			Stable[b]	[55]
Ag[e]	I	328.16	546.7	510.69 & 578.37 532	14		101–130	[10, 59] [17]
	L	328.16	421.21	532				[18, 47]
Cd	I	228.87	644.02	510.69 532	10		98–133	[13] [17]

J. Phys. G: Nucl. Part. Phys. **44** (2017) 084006

17

V Fedosseev *et al*

Table 3. (Continued.)

Element	Type of scheme[a]	λ_1 (vac) nm	λ_2 (vac) nm	λ_3 (vac) nm	Efficiency Abs. %	Efficiency Laser/ surf.	Isotopes A	Reference
In[e]	A	304.02 / 304.02 & 325.70	510.69 & 578.37 / 532	—		7	100–135	[60, 61] [18]
Sn	I	303.50	607.08	607.08	0.2			[6]
	J	301.00 / 286.30	811.40	823.68	9		105–138	[30, 62] [18, 63]
Sb	I	217.65	560.36	510.69 / 532	2.7		128–139	[53] [18]
Te	J	214.35	573.52	901.51	>18		Stable	[58]
Ba	B	350.21	653.71 / 532	—		1	Stable	[49]
	A		532					[20]
Ba$^+$	L	455.53	223.35	532	1.2[c]		Stable	[49]
Pr	I	461.90	900.00	532			Stable	[17, 47]
Nd	D	588.95	597.10	597.10		15	138–140 and stable	[15, 64]
Sm	E	600.58	675.34	676.37		6	140–143 and stable	[17, 65]
Tb	E	579.72	551.80	618.43		>1.8	149, 159	[51, 66]
Dy	D	626.08	607.66	510.69 / 532	20	50	149–164	[53] [17]
	I	418.80	776.22	532		12		
Ho	I	405.50	623.43	532	>20	60	163, 165	[18]
	J			838.36		45		
Tm	E	589.73	571.40	575.67	>2		Stable[d]	[6, 67]
Yb	E	555.80	581.23	581.23	15	20	155–178	[4, 6]
	A	267.28	532	—				[18, 47]
Au[e]	M	267.67	306.63	674.08	>3		176–198, 201, 202	[68]
Hg[e]	L	253.73	313.28	532	6		177–208	[18, 45, 49, 69]
Tl[e]	A	276.87	510.69 & 578.37 / 532	—	27	100	179–205	[51] [15]
Pb[e]	I	283.39	600.35 / 601.33	510.69 & 578.37 / 532	3		182–215	[70] [17]

Table 3. (Continued.)

Element	Type of scheme[a]	λ_1 (vac) nm	λ_2 (vac) nm	λ_3 (vac) nm	Efficiency Abs. %	Efficiency Laser/ surf.	Isotopes A	Reference
Bi[e]	I	306.86	555.36	510.69 & 578.37 532	6		187–218	[51] [18]
Po[e]	I	245.08	539.03 843.62	510.69			192–211, 216–219	[71]
		255.88	843.62	532				[15]
	K	255.88	843.62	593.94				[40]
At[e]	I	216.29	795.45 915.46	532 532			194–211, 217–219	[72] [47]
	K		795.45	617.55				
Ra	E	714.32	784.03	557.65		3	214, 222–234	[45, 55]
	G			615.28				

[a] According to notations of figure 1.
[b] Ionized in VADIS cavity.
[c] Efficiency of conversion of singly charged Ba^+ ions to the doubly charges ions Ba^{++}.
[d] Beams produced at the old SC-ISOLDE-3 facility.
[e] Elements for which isomer selective ionization has been applied.

J. Phys. G: Nucl. Part. Phys. **44** (2017) 084006

V Fedosseev *et al*

4.2. Separation of nuclear isomers

In addition to element selectivity, the RILIS offers a unique opportunity to select or enhance the fraction of a certain nuclear isomer in the produced ion beam. This is based on a sensitivity of the hyperfine structure of atomic transitions used for resonance ionization to the nuclear spins and nuclear moments. If the isomeric difference in the hyperfine structure exceeds the experimentally observed width of excitation resonance then the laser can be tuned to the specific wavelength which provides a preferential ionization of the desired nuclear state. This capability of resonance photoionization process has been demonstrated in [65] and actually applied at ISOLDE in some of the early examples of RILIS use, namely for the production of isomeric silver [59] and copper [56] beams.

Although nuclear isomerism is a rather general phenomenon, the hyperfine structure differences are not always sufficiently large as to be resolved by the RILIS lasers in the hot-cavity laser ion source conditions, where the spectral width of excitation resonances is defined by the Doppler broadening of atomic absorption lines. Therefore, the isomer selective ionization has been applied for a limited range of RILIS beams. Elements for which isomer-selective ionization has been achieved are indicated by the superscript letter (e) in table 1.

4.3. In-source RIS

As indicated in table 1, the RILIS dye and Ti:Sa lasers can be operated in a reduced line width mode. With sufficiently high resolution the ionization efficiency becomes sensitive to the isotope shift or hyperfine structure splitting. Combining this enhanced resolution with a wavelength-stabilized laser scan procedure therefore enables a spectroscopic study of these features. The laser spectra can then be analysed to extract nuclear ground state or isomer properties (charge radii and moments) and these can be charted along the isotope chain of the element of interest. Since the laser scan directly influences the ion production rate, this approach, known as in-source RIS, is the most sensitive laser spectroscopy method at ISOLDE.

The resolution of in-source RIS is limited by the Doppler broadening, $\Delta\nu_{\mathrm{D}}$ of atomic transitions inside the high temperature ionization environment, given by the following

$$\Delta\nu_{\mathrm{D}} = 7.16 \ \times 10^{-7}\nu_0(T/A)^{1/2}, \tag{12}$$

where ν_0 is the frequency of the atomic transition and A is the atomic mass number. For the heavier elements, however, the Doppler broadening approaches the line width of RILIS narrow-band lasers and, crucially, the field shift dominates the overall isotope shift and becomes comparable with the Doppler width of atomic transitions, as is illustrated in figure 7.

Thus, for elements with high Z the Doppler-limited resolution of in-source RIS enables the extraction of valuable nuclear structure information, particularly if the spectroscopic transition involves an s-electron, which experiences a greater sensitivity to nuclear changes due to its maximal wave-function overlap with the nucleus. The accuracy of spectral measurements below 100 MHz is achievable [74].

Data acquisition links with a variety of ion detection systems available at ISOLDE have been established [22, 48] to ensure laser-scan compatibility across the range of radioisotope decay modes and the abundancy distribution along an isotope chain: $(\alpha/\beta/\gamma)$ detection with the Leuven Windmill system [75]; direct ion counting with the ISOLTRAP multi-reflection time-of-flight mass separator [76]; and ion beam current measurements using the ISOLDE Faraday cups. Collectively these detection methods enable the determination of ion production rates from the nA range to as few as 0.01 ions per second [77].
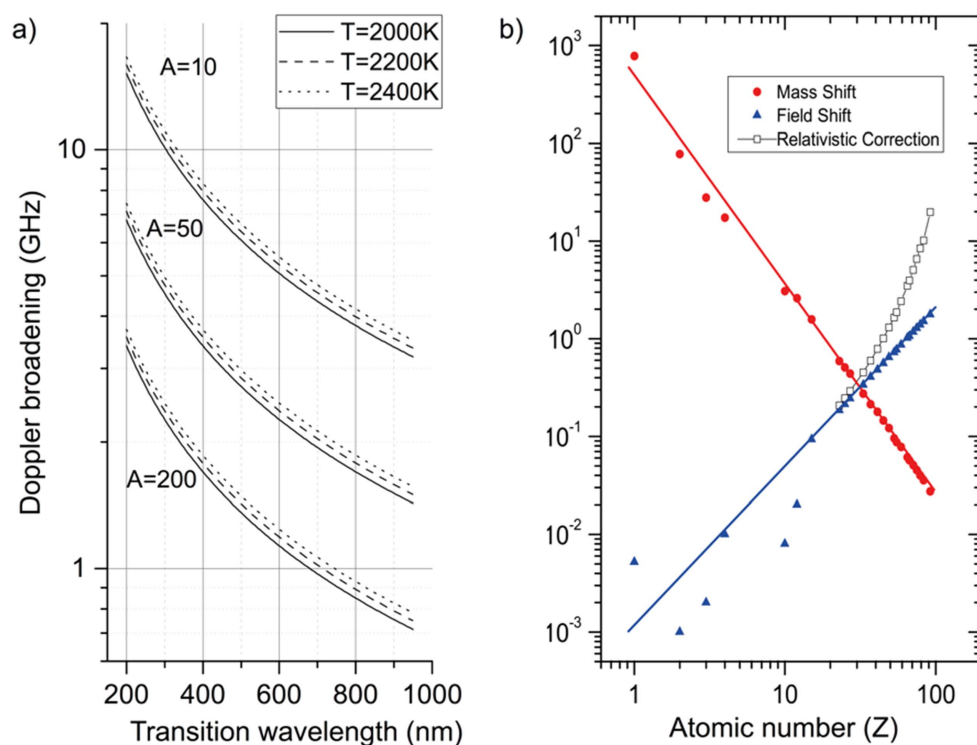
Figure 7. (a) The mass, wavelength and temperature dependence on the Doppler broadening. (b) The relative contribution of the mass shift and field shift to the total isotope shift as a function of the atomic number Z (Reproduced from [73]. 2013 The Royal Swedish Academy of Sciences. All rights reserved).

The RIS application of the RILIS is the most demanding in terms of the monitoring, control and stability requirements of the laser system. Optimizing the spectral resolution requires below-saturation laser power level for the spectroscopic transition. This means that factors such as laser beam positioning, power and pulse timing stability become critical to the acquisition of laser scans without experimentally-induced distortions. Continuous and comprehensive recording of the experimental conditions, as well as active stabilization of laser power, beam position and pulse timing synchronization has been developed to accommodate this requirement [48]. These advanced features of the RILIS installation are gradually being adopted to the benefit of increased reliability and autonomy for normal RILIS operation.

Following the series of experiments on the study of nuclear spins and electromagnetic moments of Cu isotopes [56, 78–80] the in-source RIS collaboration has performed extensive laser and nuclear-spectroscopic studies of isotopes in the lead region, namely the Tl [81], Pb [70, 82–84], Hg [45], Bi [85], Po [43, 77, 86, 87], At and Au chains [22, 88]. Our recent activity in this field has revisited the neutron-deficient Au and Hg isotopes, which were first studied at ISOLDE approximately four decades ago: the very first optical spectroscopy experiments performed at an ISOL facility [89–92]. This early work was instrumental in the discovery of the shape co-existence phenomenon and revealed two of the most striking examples of sudden nuclear shape changes in the known nuclear chart: the dramatic odd–even shape staggering of the neutron-deficient Hg isotopes, and the abrupt and pronounced shape change of the Au nuclei isotopes. The in-source spectroscopy method has brought the most

exotic isotopes available at ISOLDE within reach. By observing the return to a quasi-spherical nuclear shape as we move from the neutron mid-shell towards the proton dripline we have finally determined the end-point of these renowned features of the nuclear chart.

4.4. Other applications of the RILIS laser installation

In addition to ion beam production, the RILIS laser system offers the opportunity to exploit various laser–ion and laser–molecule interactions for the purposes of ion beam preparation and investigation. To maximize the scope for RILIS applications other than ion beam production, laser beam transport has been established to several locations in the ISOLDE hall: the ISCOOL ion beam cooler-buncher, the GANDALPH experiment, and the CRIS experimental beamline. The following is summary of the already realised and possible future applications of this additional functionality of the RILIS laser system.

ISCOOL: Laser access to the trapping region of the ISCOOL was initially established for the purposes of optical pumping of manganese ions. This technique, which was pioneered at the JYFL IGISOL facility [93], enables the preparation of the ions in a favourable state for subsequent study by collinear laser spectroscopy. The Mn ions are illuminated with laser radiation tuned to resonance with the 230.50 nm transition from the $^7S_3$ ionic ground state to the $^5P_3$ excited state at 43 370.51 cm^{-1}. The subsequent radiative decay has a non-negligible probability of populating the $^5S_2$ metastable state at 9472.97 cm^{-1}. Since the residency time of the ion cloud in the laser interaction region is long compared to the RILIS laser duty cycle, multiple laser–ion interactions are inevitable and the result is that the ion ensemble is 'pumped' into the metastable state. In this particular case, this was favourable since it enabled the subsequent collinear fluorescence laser spectroscopy to be performed [31] using a more convenient 295 nm transition from the metastable state to the $^5P_3$ state. Another possible foreseen application of this optical pumping method may be the ability to influence the probability of a subsequent charge exchange process prior to the study of a neutral atom beam by laser spectroscopy. Finally, laser beam access to ISCOOL will make possible any future investigation of laser-induced dissociation of molecular ions inside the trapping region. This may be of interest for cases where the formation of a volatile molecule is the only means of releasing the element of interest from the ISOLDE target.

GANDALPH: The GANDALPH setup is a transportable experimental beamline, initially designed to study the electron affinities of the radioactive elements astatine and polonium [94, 95]. The experiment applies the technique of laser photodetachment spectroscopy where a frequency tunable laser beam is overlapped collinearly with a beam of negative ions of the isotope to study. The neutralized fraction of the beam is detected as a function of photon energy; the electron affinity can be derived from the threshold energy of neutralization. GANDALPH was first connected to the GLM beamline and transport of one laser beam from RILIS was established. The first successful electron affinity measurement of a radioactive isotope was performed on ^{128}I. Further details on GANDALPH and the first results can be found in a dedicated article in this issue [96].

CRIS: The initial commissioning and first results obtained by the CRIS experiment relied on the frequency-doubled output from a RILIS narrow-band Ti:Sa laser, which was transmitted to the CRIS beam line via an optical fibre [97]. Scanning control of the RILIS laser was made possible by a remote interface to the shared variables of the REACT system. An additional future application of this infrastructure may be the transmission of a single mode CW laser beam from CRIS to the RILIS laboratory for pulsed amplification using the RILIS lasers. This would result in a laser with a Fourier limited line width suitable for a proposed campaign of sub-Doppler in-source spectroscopy studies [98].

5. Conclusions and outlook

Ion production by resonance laser ionization has emerged as an essential capability of modern ISOL facilities. As a result of the increased demand for laser ionized beams, the ISOLDE RILIS has undergone constant development since 1994. The modern RILIS system is now the most capable and heavily used system of its kind worldwide. The ongoing RILIS development is focused on three main areas:

Laser technologies—for improved reliability, stability, efficiency and spectral resolution (when required).

Ionization schemes—to increase efficiency and number of accessible elements.

Ion sources—for increased selectivity and/or efficiency.

The latter of these is particularly challenging due to the resources required to construct and test new innovations. For example, the LIST concept, proposed in 2003, required more than 10 years of modification and characterization until it finally became operational at ISOLDE in 2014. On the other hand, improving the ion beam intensity from an ISOL facility through ion source development is typically more cost effective than achieving the same gain through an increase in target size or driver beam intensity. Furthermore, ion source selectivity improvements not only improve experimental conditions, they also reduce the build-up of an unwanted radioactive inventory downstream of target assembly.

As was discussed in section 2.2, the high-temperature resistively heated surface ion source cavity offers the combination of simplicity and robustness, along with atom confinement and high ion survival probability which is crucial for efficient laser ion source operation with pulsed lasers. Such features are unmatched in alternative laser ion source options however the problem of thermally ionized isobaric contamination can be overwhelming for many ion beams of interest. Tackling this issue is a main focus of ongoing laser ion source R&D. The LIST has proven effective but comes at the cost of an often-unacceptable efficiency reduction. An alternative approach is to enhance and exploit the pulsed nature of the laser-ion creation. The extracted laser-ion bunch characteristics have been studied at length and the inverse proportionality of the bunch length to the longitudinal cavity voltage is documented [99]. Mishin, one of the pioneers of the laser ion source, proposed a further enhancement of this effect by allowing the laser-ions to emerge from the hot cavity inside a field-free drift-region of equal length to the cavity [100]. An ion generated at the rear of the cavity has a longer distance to travel to reach the end of the drift region than an ion generated at the cavity exit but it experiences the full cavity longitudinal voltage drop and therefore travels faster and eventually catches up with the slower ion. The result is that the ion bunch reaches a time focus at the extraction position. The ion bunch compression is limited only by the cavity voltage and turn-around time of ions with a thermal velocity component directed towards the target during the ionization. Initial studies and simulations suggest that a selectivity improvement of at least two orders of magnitude may be achievable, with little reduction in overall RILIS efficiency. The many potential pre-requisites of this project are currently under various stages of ongoing development: high resistance cavity; 10 kHz pulsed heating with duty cycle/voltage modulation; use of the LIST as a drift region; and sub microsecond fast beam gating.

Naturally, for the development of new ion beams at ISOL facilities, the target and ion source development are often intertwined. This is the case for an ongoing project aimed at the extraction of refractory transition metals from ISOLDE through the formation of weakly-bound volatile molecules. An investigation of the suitability of the RILIS lasers for molecular break-up and subsequent resonance ionization of the refractory metal atom is foreseen [101] as part of a feasibility study conducted at ISOLDE.

Finally, RIS or radioactive isotopes, the flagship of RILIS operation, is reaching an applicability limit since the prolific measurement campaign has now addressed almost all of the feasible measurement cases in the heavy-isotope region. A further-reaching exploitation of this method, for both isomer selective ionization and for nuclear structure studies, will require a means of overcoming the Doppler-broadening limitation. This can be realised through the development of a laser ion source environment with counter-propagating laser beams (achievable through the insertion of a mirror inside the ion source or transfer line). In this case, if an ionization scheme which requires a 2-photon transition is used, and this transition is accessed by a narrow linewidth (Fourier limited) injection-seeded pulsed laser, Doppler-free two-photon spectroscopy becomes possible: the Doppler shift of each atom, as seen by the incoming laser beam, is exactly compensated for by the opposite Doppler shift seen by the reflected laser beam. The first application of this method at ISOLDE for the study of silicon isotopes has already been proposed [98].

In conclusion, the RILIS has a long and successful history as an essential component of the ISOLDE ion beam production process. The subsequent adoption of the RILIS method as a key consideration for ISOL facilities worldwide is testament to this. Nevertheless, despite its over two decades of operation at ISOLDE, significant scope still remains to further develop RILIS methods for new and particularly challenging ISOLDE beams.

Acknowledgments

ORCID

Sebastian Rothe ⓘ https://orcid.org/0000-0001-5727-7754

References

[1] Letokhov V S 1987 *Laser Photoionization Spectroscopy* (Orlando, FL: Academic)
[2] Hurst G S and Payne M G 1988 *Principles and Applications of Resonance Ionization Spectroscopy* (Bristol: Hilger)
[3] Letokhov V S and Mishin V I 1984 Laser photoionization pulsed source of radioactive atoms *On-Line in 1985 and Beyond—A Workshop on the ISOLDE Programme—Abstracts (Zinal, Switzerland, 18–24 June 1984)* p D7 (http://cds.cern.ch/record/152322)
[4] Alkhazov G D, Letokhov V S, Mishin V I, Panteleyev V N, Romanov V I, Sekatsky S K and Fedoseyev V N 1989 Highly effective Z-selective photoionization of atoms in a hot metallic cavity followed by electrostatic confinement of the ions *Pis'ma Zh. Techn. Fiz.* **15** 63–6
[5] Fedoseev V N, Kudryavtsev Y A, Letokhov V S, Mishin V I, Ravn H, Sundell S, Kluge H J and Scheerer F 1991 A laser ion source for on-line separation *Resonance Ionization Spectroscopy 1990—Proc. 5th Int. Symp. on RIS and its Applications (Varese, Italy, 16–21 September 1990)* ed J E Parks and N Omenetto (Bristol: IOP) pp 129–32

[6] Scheerer F, Fedoseyev V N, Kluge H-J, Mishin V I, Letokhov V S, Ravn H L, Shirakabe Y, Sundell S and Tengblad O 1992 A chemically selective laser ion source for on-line mass separation *Rev. Sci. Instrum.* **63** 2831–3

[7] Mishin V I, Fedoseyev V N, Kluge H J, Letokhov V S, Ravn H L, Scheerer F, Shirakabe Y, Sundell S and Tengblad O 1993 Chemically selective laser ion-source for the CERN-ISOLDE on-line mass separator facility *Nucl. Instrum. Methods Phys. Res.* B **73** 550–60

[8] Alkhazov G D, Batist L K, Bykov A A, Vitman V D, Letokhov V S, Mishin V I, Panteleyev V N, Sekatsky S K and Fedoseyev V N 1991 Application of a high efficiency selective laser ion source at the IRIS facility *Nucl. Instrum. Methods Phys. Res.* A **306** 400–2

[9] Barker J 1993 Request for implementation and further development of the ISOLDE laser ion-source *Proposal to ISOLDE Committee* CERN-ISC-93-10; ISC-P-47 CERN. Geneva. ISOLDE Experiments Committee (http://cds.cern.ch/record/297272)

[10] Fedoseyev V N *et al* 1995 Study of short-lived silver isotopes with a laser ion source *Z. Phys.* A **353** 9–10

[11] Fedoseyev V N *et al* 1997 Chemically selective laser ion source of manganese *Nucl. Instrum. Methods Phys. Res.* B **126** 88–91

[12] Jokinen A *et al* 1997 Selective laser ionization of radioactive Ni-isotopes *Nucl. Instrum. Methods Phys. Res.* B **126** 95–9

[13] Lettry J *et al* 1998 Recent development of the ISOLDE laser ion source *Rev. Sci. Instrum.* **69** 761–3

[14] Fedosseev V N *et al* 2008 ISOLDE RILIS: new beams, new facilities *Nucl. Instrum. Methods Phys. Res.* B **266** 4378–82

[15] Marsh B A *et al* 2010 The ISOLDE RILIS pump laser upgrade and the LARIS laboratory *Hyperfine Interact.* **196** 129–41

[16] Rothe S, Marsh B A, Mattolat C, Fedosseev V N and Wendt K 2011 A complementary laser system for ISOLDE RILIS *Proc. Int. Nuclear Physics Conf. 2010 (Vancouver, Canada, 2010)* Rothe S, Marsh B A, Mattolat C, Fedosseev V N and Wendt K 2011 *J. Phys.: Conf. Ser.* **312** 052020

[17] Fedosseev V N *et al* 2012 Upgrade of the resonance ionization laser ion source at ISOLDE on-line isotope separation facility: new lasers and new ion beams *Rev. Sci. Instrum.* **83** 02A903

[18] Rothe S, Day Goodacre T, Fedorov D V, Fedosseev V N, Marsh B A, Molkanov P L, Rossel R E, Seliverstov M D, Veinhard M and Wendt K D A 2016 Laser ion beam production at CERN-ISOLDE: new features—more possibilities *Nucl. Instrum. Methods Phys. Res.* B **376** 91–6

[19] Fink D A *et al* 2015 On-line implementation and first operation of the laser ion source and trap at ISOLDE/CERN *Nucl. Instrum. Methods Phys. Res.* B **344** 83–95

[20] Day Goodacre T *et al* 2016 Blurring the boundaries between ion sources: the application of the RILIS inside a FEBIAD type ion source at ISOLDE *Nucl. Instrum. Methods Phys. Res.* B **376** 39–45

[21] Alkhazov G D *et al* 1992 A new highly efficient method of atomic spectroscopy for nuclides far from stability *Nucl. Instrum. Methods Phys. Res.* B **69** 517–20

[22] Marsh B A *et al* 2013 New developments of the in-source spectroscopy method at RILIS/ISOLDE *Nucl. Instrum. Methods Phys. Res.* B **317** 550–6

[23] Huyse M 1983 Ionization in a hot cavity *Nucl. Instrum. Methods* **215** 1–5

[24] Beyer G J, Herrmann E, Piotrowski A, Raiko V J and Tyrroff H 1971 A new method for rare-earth isotope separation *Nucl. Instrum. Methods* **96** 437–9

[25] Johnson P G, Bolson A and Henderson C M 1973 A high temperature ion source for isotope separators *Nucl. Instrum. Methods* **106** 83–7

[26] Latuszynski A and Raiko V I 1975 Studies of the ion source with surface-volume ionization *Nucl. Instrum. Methods* **125** 61–6

[27] Kirchner R 1981 Progress in ion source development for on-line separators *Nucl. Instrum. Methods* **186** 275–93

[28] Kirchner R 1990 On the thermoionization in hot cavities *Nucl. Instrum. Methods Phys. Res.* A **292** 203–8

[29] Schwellnus F *et al* 2009 Study of low work function materials for hot cavity resonance ionization laser ion sources *Nucl. Instrum. Methods Phys. Res.* B **267** 1856–61

[30] Fedoseyev V N, Huber G, Köster U, Lettry J, Mishin V I, Ravn H L and Sebastian V (ISOLDE Collaboration) 2000 The ISOLDE laser ion source for exotic nuclei *Hyperfine Interact.* **127** 409–16

[31] Babcock C *et al* 2016 Quadrupole moments of odd-A $^{53-63}$Mn: onset of collectivity towards $N = 40$ *Phys. Lett.* B **760** 387–92

[32] Rossel R E 2015 A distributed monitoring and control system for the laser ion source RILIS at CERN-ISOLDE *Master's Thesis* Hochschule RheinMain University of Applied Sciences Wiesbaden Rüsselsheim (https://cds.cern.ch/record/2093538)

[33] Chrysalidis K 2016 Resonance ionization spectroscopy of europium: the first application of the PISA at ISOLDE-RILIS *Master's Thesis* Johannes Gutenberg-Universität Mainz (http://cds.cern.ch/record/2227955)

[34] Rossel R E 2011 Programming of the wavelength stabilization for a titanium:sapphire laser using LabVIEW and implementation into the CERN ISOLDE RILIS measurement system *Bachelor's Thesis* Hochschule RheinMain University of Applied Sciences Wiesbaden Rüsselsheim (https://cds.cern.ch/record/1523721)

[35] Rothe S, Fedosseev V N, Kron T, Marsh B A, Rossel R E and Wendt K D A 2013 Narrow linewidth operation of the RILIS titanium: sapphire laser at ISOLDE/CERN *Nucl. Instrum. Methods Phys. Res.* B **317** 561–4

[36] Marsh B, Fedosseev V, Fink D, Day Goodacre T, Rothe S, Seliverstov M, Imai N, Sjodin M and Rossel R 2013 Suitability test of a high beam quality Nd: YVO_4 industrial laser for the ISOLDE RILIS installation *Technical Report* CERN-ATS-Note-2013-007 TECH CERN. Geneva. ATS Department (https://doi.org/10.17181/CERN.F65D.P3NR)

[37] Raeder S, Heggen H, Lassen J, Ames F, Bishop D, Bricault P, Kunz P, Mjøs A and Teigelhöfer A 2014 An ion guide laser ion source for isobar-suppressed rare isotope beams *Rev. Sci. Instrum.* **85** 033309

[38] Blaum K, Geppert C, Kluge H-J, Mukherjee M, Schwarz S and Wendt K 2003 A novel scheme for a highly selective laser ion source *Nucl. Instrum. Methods Phys. Res.* B **204** 331–5

[39] Schwellnus F 2010 Entwicklung von Ionenquellen zur Optimierung von Selektivität und Effizienz bei der resonanten Laserionisation *PhD Thesis* Johannes Gutenberg-Universität Mainz

[40] Fink D A 2014 Improving the selectivity of the ISOLDE resonance ionization laser ion source and in-source laser spectroscopy of polonium *PhD Thesis* Ruprecht-Karls-Universität Heidelberg (https://cds.cern.ch/record/1697785)

[41] Richter S 2015 Implementierung der Laserionenquellenfalle LIST bei ISOLDE und Validierung der Spezifikationen Effizienz und Selektivität *PhD Thesis* Johannes Gutenberg-Universität Mainz

[42] Fink D A *et al* 2013 First application of the laser ion source and trap (LIST) for on-line experiments at ISOLDE *Nucl. Instrum. Methods Phys. Res.* B **317** 417–21

[43] Fink D A *et al* 2015 In-source laser spectroscopy with the laser ion source and trap: first direct study of the ground-state properties of ^{217,219}Po *Phys. Rev.* X **5** 011018

[44] Penescu L, Catherall R, Lettry J and Stora T 2010 Development of high efficiency versatile arc discharge ion source at CERN ISOLDE *Rev. Sci. Instrum.* **81** 02A906

[45] Day Goodacre T 2017 Developments of the ISOLDE-RILIS for radioactive ion beam production and the results of their application in the study of exotic mercury isotopes *PhD Thesis* The University of Manchester (https://cds.cern.ch/record/2254839)

[46] Breitenfeldt M 2013 Q-values of mirror transitions for fundamental interaction studies *Tech. Proposal to the ISOLDE and Neutron Time-of-Flight Committee* CERN-INTC-2013-003; INTC-P-369 CERN. Geneva. ATS Department

[47] Rothe S 2012 An all-solid state laser system for the laser ion source RILIS and in-source laser spectroscopy of astatine at ISOLDE, CERN *PhD Thesis* Johannes Gutenberg-Universität Mainz (doi:10.17181/CERN.0HNZ.7Z6X) (http://cds.cern.ch/record/1519189)

[48] Rossel R E, Fedosseev V N, Marsh B A, Richter D, Rothe S and Wendt K D A 2013 Data acquisition, remote control and equipment monitoring for ISOLDE RILIS *Nucl. Instrum. Methods Phys. Res.* B **317** 557–60

[49] Day Goodacre T *et al* 2014 Developments for the ISOLDE resonance ionization laser ion source RILIS *ISOLDE Workshop and Users Meeting 2014 '50th Anniversary Edition' (CERN, Switzerland, 15–17 December 2014)* pp 4–5 Book of abstracts (http://indico.cern.ch/event/334117/book-of-abstracts.pdf)

[50] Fedoseyev V N 1999 The use of lasers for the selective ionization of radionuclei for RIB generation *AIP Conf. Proc.* **475** 296

[51] Köster U, Fedoseyev V N and Mishin V I 2003 Resonant laser ionization of radioactive atoms *Spectrochim. Acta* B **58** 1047–68

[52] Marsh B A, Fedosseev V N, Fink D A, Day Goodacre T, Rossel R E, Rothe S, Fedorov D V, Imai N, Seliverstov D M and Molkanov P 2014 RILIS applications at CERN/ISOLDE *Hyperfine Interact.* **227** 101–11

[53] Fedosseev V N, Marsh B A, Fedorov D V, Köster U and Tengborn E 2005 Ionization scheme development at the ISOLDE RILIS *Hyperfine Interact.* **162** 15–27

[54] Day Goodacre T, Chrysalidis K, Fedorov D V, Fedosseev V N, Marsh B A, Molkanov P L, Rossel R E, Rothe S and Seiffert C 2017 The identification of autoionizing states of atomic chromium for the resonance ionization laser ion source (RILIS) of the ISOLDE radioactive ion beam facility *Spectrochim. Acta* B **129** 58–63

[55] Day Goodacre T *et al* 2016 The ISOLDE RILIS in 2016, achievements, developments and future plans *ISOLDE Workshop and Users Meeting 2016 (CERN, Switzerland, 07–09 December 2016)* p 19 Book of abstracts (http://indico.cern.ch/event/561089/book-of-abstracts.pdf)

[56] Köster U *et al* 2000 Isomer separation of ^{70g}Cu and ^{70m}Cu with a resonance ionization laser ion source *Nucl. Instrum. Methods Phys. Res.* B **160** 528–35

[57] Zherikhin A N, Letokhov V S, Mishin V I, Muchnik M E and Fedoseyev V N 1983 Production of photoionic gallium beams through stepwise ionization of atoms by laser radiation *Appl. Phys.* B **30** 47–52

[58] Day Goodacre T, Fedorov D, Fedosseev V N, Forster L, Marsh B A, Rossel R E, Rothe S and Veinhard M 2016 Laser resonance ionization scheme development for tellurium and germanium at the dual Ti:Sa-dye ISOLDE RILIS *Nucl. Instrum. Methods Phys. Res.* A **830** 510–4

[59] Jading Y *et al* 1997 Production of radioactive Ag ion beams with a chemically selective laser ion source *Nucl. Instrum. Methods Phys. Res.* B **126** 76–80

[60] Muchnik M L, Orlov Y V, Parshin G D, Chernyak E Y, Letokhov V S and Mishin V I 1983 Generation of an indium ion beam by selective multistage laser photoionization of atoms *Sov. J. Quantum Electron.* **13** 1515–7

[61] Dillmann I *et al* 2002 Selective laser ionisation of $N \geqslant 82$ indium isotopes: the new r-process nuclide ^{135}In *Eur. Phys. J.* A **13** 281–4

[62] Scheerer F, Albus F, Ames F, Kluge H-J and Trautmann N 1992 An efficient excitation scheme for resonance ionization of tin in a laser ion source *Spectrochim. Acta* B **47** 793–7

[63] Liu Y *et al* 2006 Laser ion source tests at the HRIBF on stable Sn, Ge and Ni isotopes *Nucl. Instrum. Methods Phys. Res.* B **243** 442–52

[64] Zuzikov A D, Mishin V I and Fedoseev V N 1988 Laser resonance photoionization spectroscopy of excited and autoionization atomic states of rare-earth elements: III. Neodimium *Opt. Spectrosc.* **64** 287–8

[65] Mishin V I *et al* 1987 Resonance photoionization spectroscopy and laser separation of ^{141}Sm and ^{164}Tm nuclear isomers *Opt. Commun.* **61** 383–6

[66] Fedoseev V N, Mishin V I, Vedeneev D S and Zuzikov A D 1991 Laser resonant photoionization spectroscopy of highly excited and autoionization states of terbium atoms *J. Phys. B: At. Mol. Opt. Phys.* **24** 1575–83

[67] Mishin V I, Sekatski S K, Fedoseev V N, Buyanov N B, Letokhov V S, Alkhazov G D, Barzakh A E, Denisov V P, Ivanov V S and Chubukov I Y 1987 Ultrasensitive resonance laser photoionization spectroscopy of the radioisotope chain $^{157-172}$Tm produced by a proton accelerator *Sov. Phys.—JETP* **66** 235–42

[68] Marsh B A, Fedosseev V N and Kosuri P 2006 Development of a RILIS ionization scheme for gold at ISOLDE, CERN *Hyperfine Interact.* **171** 109–16

[69] Day Goodacre T *et al* 2017 RILIS-ionized mercury and tellurium beams at ISOLDE CERN *Hyperfine Interact.* **238** 41

[70] Andreyev A N *et al* 2002 Nuclear spins, magnetic moments and α-decay spectroscopy of long-lived isomeric states in ^{185}Pb *Eur. Phys. J.* A **14** 63–75

[71] Cocolios T E *et al* 2008 Resonant laser ionization of polonium at RILIS-ISOLDE for the study of ground- and isomer-state properties *Nucl. Instrum. Methods Phys. Res.* B **266** 4403–6

[72] Rothe S *et al* 2013 Measurement of the first ionization potential of astatine by laser ionization spectroscopy *Nat. Commun.* **4** 1835

[73] Blaum K, Dilling J and Nörtershäuser W 2013 Precision atomic physics techniques for nuclear physics with radioactive beams *Phys. Scr.* T **152** 014017

[74] Fedosseev V N, Fedorov D V, Horn R, Huber G, Köster G, Lassen J, Mishin V I, Seliverstov M D, Weissman L and Wendt K 2003 Atomic spectroscopy studies of short-lived isotopes and nuclear isomer separation with the ISOLDE RILIS *Nucl. Instrum. Methods Phys. Res.* B **204** 353–8

[75] Andreyev A N *et al* 2010 New type of asymmetric fission in proton-rich nuclei *Phys. Rev. Lett.* **105** 252502

[76] Wolf R *et al* 2012 On-line separation of short-lived nuclei by a multi-reflection time-of-flight device *Nucl. Instrum. Methods Phys. Res.* A **686** 82–90

[77] Seliverstov M D *et al* 2013 Charge radii of odd-A $^{191-211}$Po isotopes *Phys. Lett.* B **719** 362–6

[78] Weissman L *et al* 2002 Magnetic moments of ^{68}Cu^{g,m} and ^{70}Cu^{g,m1,m2} nuclei measured by in-source laser spectroscopy *Phys. Rev.* C **65** 024315

[79] Stone N J, Köster U, Rikovska Stone J, Fedorov D V, Fedoseyev V N, Flanagan K T, Haas M and Lakshmi S 2008 The magnetic dipole moments of ^{58}Cu and ^{59}Cu by in-source laser spectroscopy *Phys. Rev.* C **77** 067302

[80] Flanagan K T *et al* 2009 Nuclear spins and magnetic moments of ^{71,73,75}Cu: inversion of $\pi 2p_{3/2}$ and $\pi 1f_{5/2}$ Levels in ^{75}Cu *Phys. Rev. Lett.* **103** 142501

[81] Barzakh A E *et al* 2017 Changes in mean-squared charge radii and magnetic moments of $^{179-184}$Tl measured by in-source laser spectroscopy *Phys. Rev.* C **95** 014324

[82] De Witte H *et al* 2007 Nuclear charge radii of neutron-deficient lead isotopes beyond $N = 104$ midshell investigated by in-source laser spectroscopy *Phys. Rev. Lett.* **98** 112502

[83] Seliverstov M D *et al* 2009 Charge radii and magnetic moments of odd-A $^{183-189}$Pb isotopes *Eur. Phys. J.* A **41** 315–21

[84] Sauvage J *et al* 2009 Nuclear structure of ^{189}Tl states studied via $\beta+$/EC decay and laser spectroscopy of $^{189m+g}$Pb *Eur. Phys. J.* A **39** 33–48

[85] Barzakh A *et al* (On behalf of Leuven-Gatchina-ISOLDE-Mainz-Manchester-York and Windmill-ISOLTRAP-RILIS collaboration) 2016 Shape staggering, shape coexistence and beta-delayed fission in bismuth isotopes studied by in-source laser spectroscopy (IS608) *ISOLDE Workshop and Users Meeting 2016 (CERN, Switzerland, 07–09 December 2016)* p 2 Book of abstracts (http://indico.cern.ch/event/561089/book-of-abstracts.pdf)

[86] Cocolios T E *et al* 2011 Early onset of ground state deformation in neutron deficient polonium isotopes *Phys. Rev. Lett.* **106** 052503

[87] Seliverstov M D *et al* 2014 Electromagnetic moments of odd-A $^{193-203,211}$Po isotopes *Phys. Rev.* C **89** 034323

[88] Andreyev A N *et al* (Windmill Collaboration) 2014 *β-Delayed Fission and In-Source Laser Spectroscopy in the Lead Region Report* CERN-INTC-2014-013; INTC-SR-029 CERN. Geneva. ISOLDE and Neutron Time-of-Flight Experiments Committee

[89] Bonn J, Huber G, Kluge H-J, Kugler L and Otten E W 1972 Sudden change in the nuclear charge distribution of very light mercury isotopes *Phys. Lett.* B **38** 308–11

[90] Kühl T, Dabkiewicz P, Fischer H, Kluge H-J, Kremmling H and Otten E-W 1977 Nuclear shape staggering in very neutron-deficient Hg isotopes detected by laser spectroscopy *Phys. Rev. Lett.* **39** 180–3

[91] Ulm G *et al* 1986 Isotope shift of ^{182}Hg and an update of nuclear moments and charge radii in the isotope range ^{182}Hg–^{206}Hg *Z. Phys.* A **325** 247–59

[92] Wallmeroth K *et al* 1987 Sudden change in the nuclear distribution of very light gold isotopes *Phys. Rev. Lett.* **58** 1516–9

[93] Cheal B *et al* 2009 Laser spectroscopy of niobium fission fragments: first use of optical pumping in an ion beam cooler buncher *Phys. Rev. Lett.* **102** 222501

[94] Rothe S 2013 Preparation of negative ion beams for the determination of the electron affinity of polonium and astatine by laser photodetachment *Letter of Intent* CERN-INTC-2013-037; INTC-I-148 CERN, Geneva, ISOLDE and Neutron Time-of-Flight Experiments Committee (https://doi.org/10.17181/CERN.YJ9E.K5F5)

[95] Rothe S 2016 Determination of the electron affinity of astatine and polonium by laser photodetachment *Proposal* CERN-INTC-2016-017; INTC-P-462 CERN, Geneva, ISOLDE and Neutron Time-of-Flight Experiments Committee (https://doi.org/10.17181/CERN.OZFJ.5MKK)

[96] Rothe S *et al* 2017 Laser photodetachment of radioactive ^{128}I$^-$ *J. Phys. G: Nucl. Part. Phys.* submitted

[97] Flanagan K T *et al* 2013 Collinear resonance ionization spectroscopy of neutron-deficient francium isotopes *Phys. Rev. Lett.* **111** 212501

[98] Garcia Ruiz R F 2017 Exploring the feasibility of production and laser spectroscopy experiments of exotic silicon isotopes *Letter of Intent* CERN-INTC-2017-026; INTC-I-176 CERN. Geneva. ISOLDE and Neutron Time-of-Flight Experiments Committee

[99] Lettry J, Catherall R, Köster U, Georg U, Jonsson O, Marzari S and Fedosseev V 2003 Alkali suppression within laser ion-source cavities and time structure of the laser ionized ion-bunches *Nucl. Instrum. Methods Phys. Res.* B **204** 363–7

[100] Mishin V I, Malinovsky A L and Mishin D V 2009 Resonant ionization laser ion source (RILIS) with improved selectivity achieved by ion pulse compression using in-source time-of-flight technique *AIP Conf. Proc.* **1104** 207

[101] Seiffert C and Ballof J 2017 Extraction of refractory elements by laser induced breakup and ionisation of Molybdenum Carbonyls *Letter of Intent* CERN-INTC-2017-031; INTC-I-178 CERN, Geneva, ISOLDE and neutron Time-of-Flight Experiments Committee (https://cds. cern.ch/record/2241995)